ELSEVIER

Journal of Organometallic Chemistry 582 (1999) 45–52

Journal of Organo metallic Chemistry

Preparation of single-source precursors to nanocrystalline gallium arsenide and gallium antimonide. X-ray crystal structures of $[Et_2GaAs(SiMe_3)_2]_2$, $[Et_2GaSb(SiMe_3)_2]_2$ and $Et_2\overline{GaAs(SiMe_3)_2Ga(Et)_2Sb}(SiMe_3)_2$ ☆

Edward E. Foos [a], Richard J. Jouet [a], Richard L. Wells [a,*], Arnold L. Rheingold [b], Louise M. Liable-Sands [b]

[a] *Department of Chemistry, Paul M. Gross Chemical Laboratory, Duke University, Durham, NC 27708, USA*
[b] *Department of Chemistry, Drake Hall, University of Delaware, Newark, DE 19716, USA*

Received 9 September 1998

Abstract

The 1:1 mole ratio reaction of Et_2GaCl with $As(SiMe_3)_3$ leads to the isolation of $[Et_2GaAs(SiMe_3)_2]_2$ (**1**), while the analogous reaction with $Sb(SiMe_3)_3$ results in the formation of $[Et_2GaSb(SiMe_3)_2]_2$ (**2**). The mixed-pnicogen compound $Et_2\overline{GaAs(SiMe_3)_2Ga(Et)_2Sb}(SiMe_3)_2$ (**3**) was obtained from both the equilibration of **1** and **2**, as well as the 2:1:1 mole ratio reaction of Et_2GaCl with $As(SiMe_3)_3$ and $Sb(SiMe_3)_3$. X-ray crystal structures are reported for **1**, **2** and **3**, as well as a variable temperature ^1H-NMR study of **2** and **3**. The dimer **2** was found to exhibit a dimer/trimer equilibrium in solution. Thermolysis of all three compounds results in the formation of GaAs, GaSb or $GaAs_xSb_{(1-x)}$ through a β-hydride elimination pathway.

Keywords: Precursors; Nanocrystalline; Gallium arsenide; Gallium antimonide; Gallium arsenide antimonide

---

1. Introduction

Much of the recent research in our laboratory has focused on the synthesis and characterization of single-source precursors to binary Group 13–Group 15 materials, with particular emphasis on gallium containing species that can be utilized as precursors to GaN, GaP, GaAs and GaSb [1]. Thermolysis of several of these potential precursors has resulted in the formation of the desired nanocrystalline gallium pnictide semiconductor materials through several different routes; namely dehalosilylation [2], deamination [3], or β-hydride elimination [4].

While much effort has been placed on the synthesis of precursors to GaP and GaAs, far less effort has been directed toward compounds that could serve as precursors to GaSb. For example, prior to our investigations, the only X-ray crystal structures containing a direct Ga–Sb bond to be reported in the literature were $[Cl_2GaSb(t\text{-}Bu)_2]_3$ [5] and $[Me_2GaSb(t\text{-}Bu)_2]_3$ [6]. We have recently prepared several such compounds [4,7], and found that the dimer $[t\text{-}Bu_2GaSb(SiMe_3)_2]_2$ produces nanocrystalline GaSb through a β-hydride elimination pathway [4]. Additionally, the GaSb produced from this thermolysis is of higher purity than the material obtained from dehalosilylation reactions [2d]. In light of these results, we were interested in exploring other systems to see if such an elimination pathway could be observed not only for other small alkyl groups bound to the Group 13 metal, but also for precursors containing pnicogen atoms other than antimony.

☆ Dedicated to Professor Alan H. Cowley on the occasion of his 65th birthday.

* Corresponding author.

PII: S0022-328X(98)01184-X

Conspicuously absent from the aforementioned studies are compounds that could serve as precursors to gallium containing ternary materials, the only examples of which are $I_2GaP(SiMe_3)_2Ga(I)_2As(SiMe_3)_2$ [8] and $Ga_2(As/P)Cl_3$ [9]. Thermolysis studies on these compounds suggested that they could be used for the formation of $GaP_xAs_{(1-x)}$. In spite of this, only two other examples of compounds containing a 'mixed-pnicogen' central ring similar to $I_2GaP(SiMe_3)_2Ga(I)_2As(SiMe_3)_2$ exist, one containing aluminum [10] and the other indium [11]. In all three cases, the pnicogen atoms incorporated into the material are phosphorus and arsenic. Thus, preparation of a mixed-pnicogen compound containing antimony would make an excellent target for our synthetic efforts.

In an attempt to explore these areas, herein we report the synthesis and characterization of the dimeric compounds $[Et_2GaAs(SiMe_3)_2]_2$ (**1**) and $[Et_2GaSb(SiMe_3)_2]_2$ (**2**), as well as the mixed-pnicogen compound $Et_2GaAs(SiMe_3)_2Ga(Et)_2Sb(SiMe_3)_2$ (**3**). X-ray crystal structures are presented for all three compounds. In addition, the thermolysis behaviors of **1**, **2** and **3** have been examined in an attempt to judge their utility as precursors to GaAs, GaSb and $GaAs_xSb_{(1-x)}$.

2. Experimental

2.1. General considerations

All manipulations of air- and moisture-sensitive materials were performed in a Vacuum Atmospheres HE-493 Dri-Lab containing an argon atmosphere or by standard Schlenk techniques. Solvents were distilled from sodium/potassium alloy under dry dinitrogen. $As(SiMe_3)_3$ [12] and $Sb(SiMe_3)_3$ [13] were prepared from literature methods. Et_3Ga and $GaCl_3$ were purchased from Strem Chemicals and used as received. Et_2GaCl was obtained from the 2:1 comproportionation reaction of Et_3Ga with $GaCl_3$. All ^1H and $^{13}C\{^1H\}$ spectra were recorded on a Varian Inova 400 NMR spectrometer operating at 399.948 and 100.577 MHz, respectively, in 5 mm tubes, septum-sealed under argon. Spectra were referenced to TMS using the residual protons or carbons of deuterotoluene at δ 2.09 or 20.4, respectively, or deuterobenzene at δ 7.15 or 128.0, respectively. Melting points (uncorrected) were obtained with a Thomas-Hoover Uni-melt apparatus, using capillaries that were flame-sealed under argon. Elemental analyses were performed by E + R Microanalytical Laboratory, Inc., Corona, NY. Powder X-ray diffraction (XRD) data were collected on a Phillips XRG-3000 diffractometer utilizing Cu–K_α radiation. IR spectra of volatile gases were acquired using a gas cell on a BOMEM Michelson MB-100 FT-IR spectrometer. Single-crystal X-ray diffraction studies were performed at the University of Delaware on a Siemens P4/CCD diffractometer.

2.2. Synthesis of $[Et_2GaAs(SiMe_3)_2]_2$ (**1**)

A 100 ml round bottom flask equipped with a stirbar and a Teflon valve was charged with Et_2GaCl (0.327 g; 2.0 mmol) and 10 ml of hexane. A solution of $As(SiMe_3)_3$ (0.589 g; 2.0 mmol) in 10 ml hexane was then added via pipet at room temperature in a dry box. The flask was sealed and removed from the dry box and the clear, colorless solution stirred for 12 h. The volume of the solution was reduced in vacuo, and storage at − 30°C for 1 day afforded colorless crystals of **1** (0.624 g, 89% yield). M.p.: 192–202°C. Anal. Calc. (found) for $Ga_2As_2Si_4C_{20}H_{56}$: C, 34.40 (34.33); H, 8.08 (8.27). ^1H-NMR: δ 0.42 (s, 36H, $-SiMe_3$), δ 0.95 [q, 8H, $-CH_2CH_3$ (J_{H-H} = 8.0 Hz)], δ 1.34 [t, 12H, $-CH_2CH_3$ (J_{H-H} = 8.0 Hz)]. $^{13}C\{^1H\}$-NMR: δ 4.65 (s, $-SiMe_3$), δ 8.61 (s, $-CH_2CH_3$), δ 10.94 (s, $-CH_2CH_3$).

2.3. Synthesis of $[Et_2GaSb(SiMe_3)_2]_2$ (**2**)

A 250 ml round bottom flask equipped with a stirbar and a Teflon valve was charged with Et_2GaCl (0.245 g; 1.5 mmol) and 20 ml of hexane. A solution of $Sb(SiMe_3)_3$ (0.541 g; 1.5 mmol) in 20 ml hexane was then added via pipet at room temperature in a dry box. The flask was sealed and removed from the dry box and the clear, yellow solution stirred for 12 h. The volume of the solution was reduced in vacuo, and storage at − 30°C for 1 day afforded thick, colorless needles of **2** (0.334 g, 56% yield). M.p.: 147–157°C (decomposed to black liquid). Anal. Calc. (found) for $Ga_2Sb_2Si_4C_{20}H_{56}$: C, 30.33 (30.61); H, 7.13 (7.08). ^1H-NMR: δ 0.50 (s, dimer, $-SiMe_3$), δ 0.57 (s, trimer, $-SiMe_3$), δ 1.05 [q, dimer, $-CH_2CH_3$ (J_{H-H} = 8.0 Hz)], δ 1.09 [q, trimer, $-CH_2CH_3$ (J_{H-H} = 8.0 Hz)], δ 1.41 [t, dimer, $-CH_2CH_3$ (J_{H-H} = 8.0 Hz)], δ 1.46 [t, trimer, $-CH_2CH_3$ (J_{H-H} = 8.0 Hz)]. $^{13}C\{^1H\}$-NMR: δ 5.37 (s, dimer, $-SiMe_3$), δ 5.73 (s, trimer, $-SiMe_3$), δ 9.19 (s, dimer/trimer, $-CH_2CH_3$), δ 12.22 (s, dimer, $-CH_2CH_3$), δ 12.46 (s, trimer, $-CH_2CH_3$).

2.4. Variable temperature ^1H-NMR study of **2**

Approximately 0.015 g of **2** was dissolved in 0.6 ml of deuterobenzene and flame sealed under reduced pressure in a 5 mm NMR tube. Spectra were taken at 25, 50, 65 and again at 25°C. All peaks returned to their original states upon cooling to 25°C. ^1H-NMR (65°C): δ 0.51 (s, 18 H, $SiMe_3$), δ 1.03 [q, 4 H, $-CH_2CH_3$ (J_{H-H} = 8 Hz)], δ 1.38 [t, 6 H, $-CH_2CH_3$ (J_{H-H} = 8 Hz)]. All peaks correspond to the dimeric $[Et_2GaSb(SiMe_3)_2]_2$ (**2**) at 65°C.

2.5. Variable concentration ^1H-NMR study of **2**

Sealed 5 mm NMR tubes containing four different concentrations of **2** in deuterobenzene [(A) 0.007/*n* M, (B) 0.033/*n* M, (C) 0.075/*n* M, (D) 0.114/*n* M] were prepared and spectra taken at 25°C. The ratios of dimer to trimer were obtained from the $SiMe_3$ peaks by integration. The identities of dimer and trimer were confirmed by the slope (1.24 ± 0.05) of the plot of the natural logarithm of the integral fractions of the dimer peaks times the total concentration (in monomeric units) versus the same for the trimer peaks.

2.6. Synthesis of $Et_2GaAs(SiMe_3)_2Ga(Et)_2Sb(SiMe_3)_2$ (**3**). Method A

A 250 ml round bottom flask equipped with a stirbar and a Teflon valve was charged with **1** (0.121 g; 0.35 mmol) and 20 ml of hexane. A solution of **2** (0.137 g; 0.35 mmol) in 20 ml hexane was then added via pipet at room temperature in a dry box. The flask was sealed and removed from the dry box and the clear, orange solution was stirred for 5 days. The volume of the solution was then reduced in vacuo, and storage at −30°C for 1 day afforded thick, colorless blocks of **3** (0.334 g, 56% yield). M.p.: 173–180°C (decomposed to black liquid). Anal. Calc. (Found) for $Ga_2AsSbSi_4C_{20}H_{56}$: C, 32.24 (32.16); H, 7.58 (7.86). ^1H-NMR: δ 0.41 (s, $-As(Si\mathit{Me}_3)_2$), δ 0.51 (s, $-Sb(Si\mathit{Me}_3)_2$), δ 1.01 [q, $-\mathit{CH}_2CH_3$ ($J_{H-H} = 8.0$ Hz)], δ 1.39 [t, $-CH_2\mathit{CH}_3$ ($J_{H-H} = 8.0$ Hz)]. $^{13}C\{^1H\}$-NMR: δ 4.56 (s, $-As(Si\mathit{Me}_3)_2$), δ 5.44 (s, $-Sb(Si\mathit{Me}_3)_2$), δ 9.07 (s, $-\mathit{CH}_2CH_3$), δ 11.59 (s, $-CH_2\mathit{CH}_3$).

2.7. Synthesis of $Et_2GaAs(SiMe_3)_2Ga(Et)_2Sb(SiMe_3)_2$ (**3**). Method B

A 100 ml round bottom flask equipped with a stirbar and a Teflon valve was charged with Et_2GaCl (0.327 g; 2.0 mmol) and 10 ml of hexane. A solution of $As(SiMe_3)_3$ (0.294 g; 1.0 mmol) and $Sb(SiMe_3)_3$ (0.341 g; 1.0 mmol) in 10 ml hexane was added via pipet at room temperature in a dry box. The flask was sealed and removed from the dry box and the clear, yellow solution was stirred for 4 days in the dark. The volume of the solution was reduced in vacuo, and storage at −30°C for 1 day afforded thick, colorless blocks of **3** (0.468 g, 63% yield).

2.8. Variable temperature ^1H-NMR study of **3**

Approximately 0.020 g of **3** was dissolved in 0.6 ml of deuterotoluene and flame sealed under reduced pressure in a 5 mm NMR tube. Spectra were taken at 25, 60, 70, 80, 90, 95 and again at 25°C. All peaks returned to their original states upon cooling to 25°C. The temperature was then reduced to 10 and 0°C, followed by warming to 25°C. No changes were observed in any of the low-temperature spectra. Due to the complexity of the downfield signals in the ethyl region, the trimethylsilyl peaks were used for the identification of species. ^1H-NMR (25°C, trimethylsilyl region): δ 0.41 (s, **3**), δ 0.42 (s, **1**), δ 0.50 (s, **2**), δ 0.51 (s, **3**), δ 0.57 (s, **2**). ^1H-NMR (80°C, trimethylsilyl region): δ 0.41 (s, **3**), δ 0.42 (s, **1**), δ 0.51 (s, **2** and **3**). ^1H-NMR (95°C, trimethylsilyl region): δ 0.42 (bs, **1** and **3**), δ 0.51 (s, **2** and **3**).

2.9. Thermolysis of **1**

1 (0.994 g, 2.84 mmol based on the monomeric unit) was loaded into a sublimator fitted with a collection trap. The entire system was evacuated for 10 min. The collection trap was cooled to −196°C and the sublimator was heated to 400°C for 5 h under static vacuum. During this time significant sublimation of **1** (later identified by ^1H- and $^{13}C\{^1H\}$-NMR spectroscopy) was observed as white crystals that formed on the walls of the sublimator above the heat source. A dark gray metallic mirror formed on the sides of the sublimator as well as the cold finger during thermolysis. This material was scraped from the sides and collected (0.072 g, 17.5%) and its identity verified by comparison of the d-spacings and line intensities obtained by XRD analysis with those of GaAs (JCPDS file 14-450). The approximate average particle size of 9 nm was calculated using the Scherrer equation [14]. The trapped volatiles were analyzed by IR spectroscopy with the following results: non-condensable CH_4 and H_2, a small non-quantifiable amount was detected; condensable $HSiMe_3$ and ethylene, approximately 2.31 mmol total. Anal. Calc. (Found) for GaAs: Ga, 48.20 (47.65); As, 51.80 (51.13); C, 0.00 (0.96); H, 0.00 (0.25). The Ga:As ratio was 1.00:1.00.

2.10. Thermolysis of **2**

Thermolysis of **2** (0.508 g, 1.3 mmol) was identical to the procedure described for compound **1**. Similar to **1**, significant sublimation of $[Et_2GaSbSiMe_3)_2]_2$ (later identified by ^1H-NMR spectroscopy) was observed as white crystals that formed on the walls of the sublimator above the heat source. The material, GaSb, formed as a metallic mirror on the sides of the sublimator during thermolysis. This material was scraped from the sides and collected (0.050 g, 20%) and its identity verified by comparison of the d-spacings and line intensities obtained by XRD analysis with those of GaSb (JCPDS file 7-215). The approximate average particle size of 10 nm was calculated using the Scherrer equation [14]. The trapped volatiles were analyzed by IR spectroscopy with the following results: non-condens-

Table 1
Crystallographic data for $[Et_2GaAs(SiMe_3)_2]_2$ (**1**), $[Et_2GaSb(SiMe_3)_2]_2$ (**2**) and $Et_2\overline{GaAs(SiMe_3)_2Ga(Et)_2Sb}(SiMe_3)_2$ (**3**)

	(**1**)	(**2**)	(**3**)
Formula	$C_{20}H_{56}As_2Ga_2Si_4$	$C_{20}H_{56}Ga_2Sb_2Si_4$	$C_{20}H_{56}AsGa_2SbSi_2$
Formula weight	698.29	791.95	745.12
Temperature (K)	198(2)	198(2)	198(2)
Radiation (Mo–K_α, λ (Å))	0.71073	0.71073	0.71073
Crystal color, habit	Colorless block	Colorless block	Colorless plate
Space group	*C*2/*c*	*C*2/*c*	*C*2/*c*
Unit cell dimensions			
a (Å)	18.1366(2)	18.3084(6)	18.1363(7)
b (Å)	9.4447(2)	9.6841(3)	9.4925(4)
c (Å)	20.4050(3)	20.8825(7)	20.5474(8)
β (°)	100.2409(11)	98.6786(7)	99.852(2)
V (Å^3)	3439.57(11)	3677.6(3)	3485.2(4)
Z	4	4	4
$D_{calc.}$ (g cm^{-3})	1.348	1.430	1.420
μ(Mo–K_α) (cm^{-1})	36.22	30.29	33.91
Diffractometer	Siemens P4/CCD	Siemens P4/CCD	Siemens P4/CCD
R(*F*) %[a]	3.78	3.46	3.70
R(*wF*^{2}) %[a]	8.75	7.93	8.66

[a] Quantity minimized $= R(wF^2) = \Sigma\,[w(F_o^2 - F_c^2)^2]/\Sigma\,[(wF_o^2)^2]^{1/2}$; $R = \Sigma\,\Delta/\Sigma\,(F_o)$, $\Delta = |(F_o - F_c)|$.

able CH_4 and H_2, 0.00 mmol; condensable $HSiMe_3$ and ethylene, ca. 1.51 mmol total. Anal. Calc. (Found) for GaSb: Ga, 36.41 (35.59); C, 0.00 (1.73); H, 0.00 (0.30).

2.11. Thermolysis of 3

Thermolysis of **3** (0.366 g, 0.491 mmol) was conducted according to the procedure described for compound **1**. Similar to both **1** and **2**, significant sublimation of **3** (later identified by ^{1}H- and $^{13}C\{^1H\}$-NMR spectroscopy) was observed as white crystals that formed on the walls of the sublimator above the heat source. The material, $GaAs_xSb_{(1-x)}$, formed as a metallic mirror on the sides of the sublimator as well as on the cold finger during thermolysis. This material was scraped from the sides and collected (0.030 g, 18.2%) and its identity verified by comparison of the d-spacings and line intensities obtained by XRD analysis with those of both GaAs (JCPDS file 14-450) and GaSb (JCPDS file 7-215). The approximate average particle size of 5 nm was calculated using the Scherrer equation [14]. The trapped volatiles were analyzed by IR spectroscopy with the following results: non-condensable CH_4 and H_2, 0.00 mmol; condensable $HSiMe_3$ and ethylene, ca. 0.87 mmol total. Anal. Calc. (Found) for $GaAs_xSb_{(1-x)}$: Ga, 41.48 (40.79); As, 22.29 (21.75); C, 0.00 (1.16); H, 0.00 (0.28).

2.12. X-ray structural solution and refinement

Crystal data collection and refinement parameters are given in Table 1, while selected bond lengths and angles are presented in Table 2. ORTEP diagrams showing the solid state conformation of **1**–**3** can be found in Figs. 1–3, respectively. The systematic absences in the diffraction data are consistent for the C-centered monoclinic space groups, *Cc* and *C*2/*c*. The *E*-statistic suggested the centrosymmetric space group, which yielded chemically reasonable and computationally stable results of refinement. The structures were solved using direct methods, completed by subsequent difference Fourier syntheses and refined by full-matrix least-squares procedures. The molecules for all three structures lie on two fold rotation axes. There is crystallographically imposed disorder between the arsenic and antimony atoms of **3**; the unique atom was refined as an undersized antimony atom and labeled PN(1). All non-hydrogen atoms were refined with anisotropic displacement coefficients and the hydrogen atoms were treated as idealized contributions. All software and sources of the scattering factors are contained in the SHELXTL (5.1) program library (G. Sheldrick, Siemens XRD, Madison, WI).

3. Results and discussion

The 1:1 mole ratio reaction of Et_2GaCl with $As(SiMe_3)_3$ leads to the isolation of the dimeric compound $[Et_2GaAs(SiMe_3)_2]_2$ (**1**), while the analogous reaction with $Sb(SiMe_3)_3$ leads to the formation of $[Et_2GaSb(SiMe_3)_3]_2$ (**2**). Equilibration of **1** and **2** in hexane solution for 5 days resulted in the formation of the mixed-pnicogen compound $Et_2\overline{GaAs(SiMe_3)_2Ga(Et)_2Sb}(SiMe_3)_2$ (**3**). It was also possible to prepare **3** from a direct reaction, that of Et_2GaCl with one-half equivalent each of $As(SiMe_3)_3$ and $Sb(SiMe_3)_3$. Both of these methods have been

Table 2
Selected bond lengths (Å) and angles (°) for $[Et_2GaAs(SiMe_3)_2]_2$ (**1**), $[Et_2GaSb(SiMe_3)_2]_2$ (**2**) and $Et_2GaAs(SiMe_3)_2Ga(Et)_2Sb(SiMe_3)_2$ (**3**)[a]

Compound **1**			
Bond lengths			
Ga(1)–As(1)	2.5429 (6)	Ga (1)–C(9)	2.002(4)
Ga(1A)–As(1)	2.5434 (6)	As(1)–Si(1)	2.3588(11)
Ga(1)–C(7)	2.013 (3)	As(1)–Si(2)	2.3609(11)
Bond angles			
Ga(1)–As(1)–Ga(1A)	92.229(19)	Si(1)–As(1)–Ga(1)	111.19(3)
As(1)–Ga(1)–As(1A)	87.771(19)	Si(1)–As(1)–Ga(1A)	114.29(4)
C(9)–Ga(1)–As(1)	113.90(12)	Si(2)–As(1)–Ga(1)	116.92(4)
C(9)–Ga(1)–As(1A)	113.47(12)	Si(2)–As(1)–Ga(1A)	114.36(3)
C(7)–Ga(1)–As(1)	110.77(12)	C(9)–Ga(1)–C(7)	115.97(19)
C(7)–Ga(1)–As(1A)	111.69(13)	Si(1)–As(1)–Si(2)	107.51(4)
Compound **2**			
Bond lengths			
Ga(1)–Sb(1)	2.7175(4)	Ga (1)–C(9)	1.993(4)
Ga(1A)–Sb(1)	2.7285(4)	Sb(1)–Si(1)	2.5586(10)
Ga(1)–C(7)	1.997(4)	Sb(1)–Si(2)	2.5587(9)
Bond angles			
Ga(1)–Sb(1)–Ga(1A)	92.726(11)	Si(1)–Sb(1)–Ga(1)	109.72(3)
Sb(1)–Ga(1)–Sb(1A)	87.274(11)	Si(1)–Sb(1)–Ga(1A)	114.22(2)
C(9)–Ga(1)–Sb(1)	113.29(12)	Si(2)–Sb(1)–Ga(1)	116.37(3)
C(9)–Ga(1)–Sb(1A)	112.11(10)	Si(2)–Sb(1)–Ga(1A)	116.60(2)
C(7)–Ga(1)–Sb(1)	111.50(13)	C(9)–Ga(1)–C(7)	117.7(2)
C(7)–Ga(1)–Sb(1A)	111.03(11)	Si(1)–Sb(1)–Si(2)	106.86(3)
Compound 3			
Bond lengths			
Ga(1)–PN(1)	2.5901(5)	Ga (1)–C(9)	2.990(4)
Ga(1A)–PN(1)	2.5889(5)	PN(1)–Si(1)	2.4089(11)
Ga(1)–PN(1A)	2.5888(5)	PN(1)–Si(2)	2.4055(11)
Ga(1)–C(7)	1.988(4)		
Bond angles			
Ga(1)–PN(1)–Ga(1A)	92.309(15)	Si(1)–PN(1)–Ga(1)	110.74(3)
PN(1)–Ga(1)–PN(1A)	87.690(15)	Si(1)–PN(1)–Ga(1A)	114.34(3)
C(9)–Ga(1)–PN(1)	113.88(13)	Si(2)–PN(1)–Ga(1)	116.82(3)
C(9)–Ga(1)–PN(1A)	112.90(13)	Si(2)–PN(1)–Ga(1A)	114.90(3)
C(7)–Ga(1)–PN(1)	110.58(13)	C(9)–Ga(1)–C(7)	116.37(16)
C(7)–Ga(1)–PN(1A)	112.01(13)	Si(1)–PN(1)–Si(2)	107.39(4)

[a] PN is the As/Sb disordered atom.

utilized in the formation of other known mixed-pnicogen ring systems [8,10,11], however, **3** represents the first example of such a compound containing a core ring other than M–P–M–As (where M = Al, Ga or In). The reactions employed in the formation of **1**, **2** and **3** are summarized in Scheme 1.

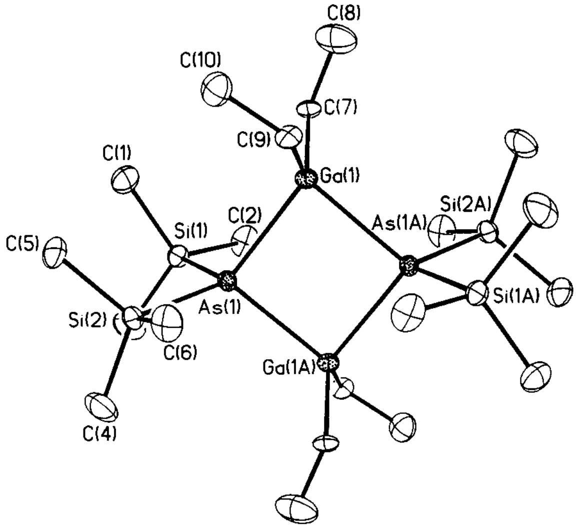

Fig. 1. ORTEP diagram of $[Et_2GaAs(SiMe_3)_2]_2$ (**1**) showing atom labeling scheme. Thermal ellipsoids at 30% probability and hydrogen atoms are omitted for clarity.

Compounds **1**, **2** and **3** are isomorphous and crystallize in the monoclinic space group *C*2/*c*. The average Ga–As bond length of 2.5432(6) Å and the Ga–As–Ga and As–Ga–As endocyclic ring angles of 92.229(19)° and 87.771(19)°, respectively, of **1** fall well within the range of values associated with the numerous gallium–arsenic dimeric compounds in the literature. For example, **1** is structurally similar to the recently reported dimeric compound $[(vinyl)_2GaAs(t\text{-}Bu)_2]_2$ [15], which contains a Ga–As bond length of 2.527(1) Å and endocyclic bond angles of 94.6(1)° (Ga–As–Ga) and 85.4(1)° (As–Ga–As). The dimeric compound $[t\text{-}Bu_2GaAs(SiMe_3)_2]_2$ [16] exhibits a Ga–As bond length of 2.630(1) Å and Ga–As–Ga and As–Ga–As bond angles of 94.85(3)° and 85.15(3)°, respectively, while the analogous average values for $[(Me_3SiCH_2)_2GaAs(SiMe_3)_2]_2$ [17] are 2.57 Å, 93.91° and 86.09°. While steric differences in the ligands bound to the metal centers no doubt influence these values, it is interesting to note that the endocylic ring angles in **1** differ by ca. 2° from these other compounds. The average Ga–Sb bond length of 2.7230(4) Å in **2** is also quite typical, although the number of structurally

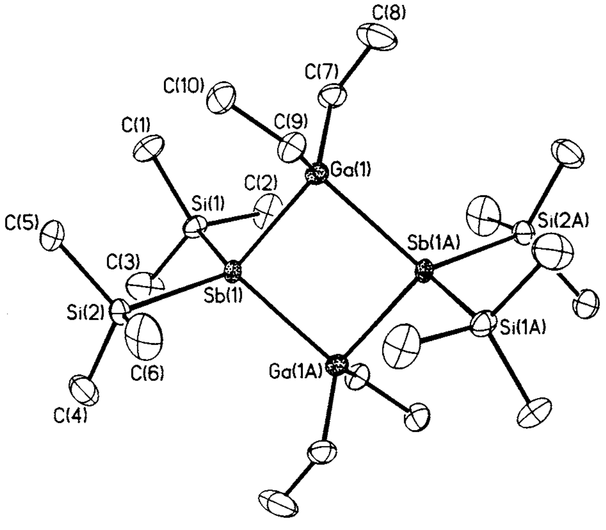

Fig. 2. ORTEP diagram of $[Et_2GaSb(SiMe_3)_2]_2$ (**2**) showing atom labeling scheme. Thermal ellipsoids at 30% probability and hydrogen atoms are omitted for clarity.

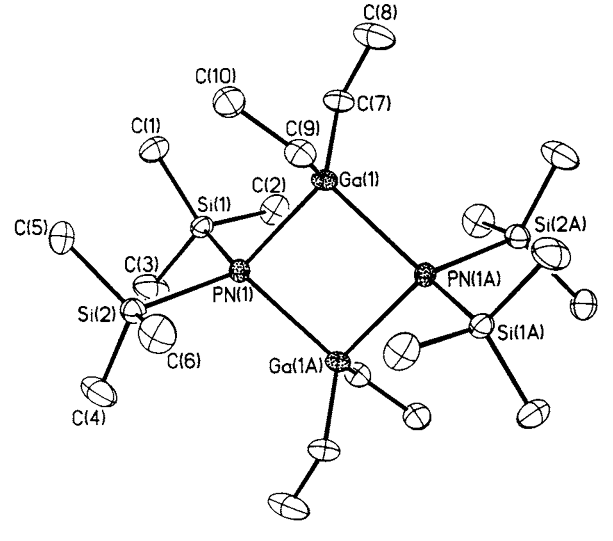

Fig. 3. ORTEP diagram of $Et_2GaAs(SiMe_3)_2Ga(Et)_2Sb(SiMe_3)_2$ (**3**) showing atom labeling scheme. The As/Sb disordered atom is labeled as PN(1). Thermal ellipsoids at 30% probability and hydrogen atoms are omitted for clarity.

characterized gallium–antimony compounds is far less than in the case of gallium–arsenic compounds, and compares well with the average length of 2.7666(7) Å found in the related compound $[t\text{-}Bu_2GaSb(SiMe_3)_2]_2$ [4]. The Ga–Sb–Ga and Sb–Ga–Sb endocyclic bond angles of 92.726(11)° and 87.274(11)°, respectively, in **2** are also similar to the analogous angles in $[t\text{-}Bu_2GaSb(SiMe_3)_2]_2$ of 94.5° and 85.5°. Presumably, the slight differences in these values are due to the significantly reduced steric bulk of the ethyl groups present in **2**.

As with the other mixed-pnicogen compounds that have been reported in the literature, **3** exhibits a 50/50 occupancy of the ring pnicogen atoms. Thus, X-ray crystallography is unable to distinguish between two different possibilities: discreet mixed-pnicogen molecules or a 50/50 co-crystallization of the dimers **1** and **2**. The existence of the mixed-pnicogen compound is supported by the NMR data (vide infra), as well as the fact that an exact cocrystallization of dimers in four separate instances seems highly improbable. The average Ga–PN (where PN is the As/Sb disordered atom) bond length of 2.5895(5) Å in **3** is less than the average of the Ga–As and Ga–Sb bond lengths in **1** and **2**. In the previously reported Al, Ga and In mixed-pnicogen compounds, which were structurally characterized [8,10,11], the metal–pnicogen bond length was essentially the average of the lengths of the starting dimers. Similarly, the Ga–PN–Ga bond angle of 92.309(15)° and the PN–Ga–PN bond angle of 87.690(15)° also deviate from the average and lie closer to the values of the analogous angles in **1**.

Interestingly, **2** appears to exhibit a dynamic process in solution, and the room temperature ^{1}H-NMR spectra is more complex than the expected singlet–quartet–triplet pattern predicted on the basis of a dimeric structure. In an effort to determine the process at work, a variable temperature ^{1}H-NMR study was performed as well as a concentration study on several samples of **2**. The singlets arising from the $-SiMe_3$ groups were used in these studies, due to the complexity of the overlapping signals in the ethyl region of the spectra. At 25°C, there were two singlets present in this region at δ 0.50 and δ 0.57, in a ratio of 2:1. As the temperature was raised from 25 to 65°C, the set of peaks associated with the singlet at δ 0.57 began to lose intensity, and a well-defined quartet and triplet (arising from the ethyl groups) were present downfield at δ 1.03 (q) and δ 1.38 (t). Upon cooling to 25°C, the second set of peaks returned and the spectra was identical to the first. Based on this behavior, it is possible to rule out an elimination process for **2** in solution, since such a process would not be expected to be reversible. Similar results were obtained from the concentration study, and the intensities of the set of peaks associated with the singlet at δ 0.57 increased with an increase in concentration. Because these peaks favored both higher concentrations and lower temperatures, they were assigned to the more associated species in solution. Combining this information with the slope of a ln/ln plot of the data that was obtained from the concentration studies, the solution behavior of **2** was attributed to a dimer/trimer equilibrium. Such an assignment finds the dimer to be the predominant species at room temperature, and indeed the X-ray crystal structure of this compound indicates that it is dimeric in the solid state (vide supra).

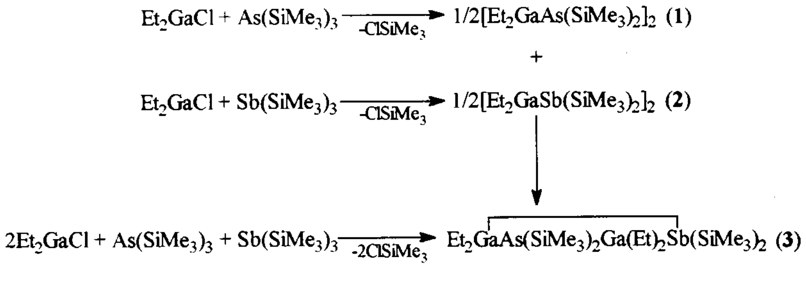

Scheme 1.

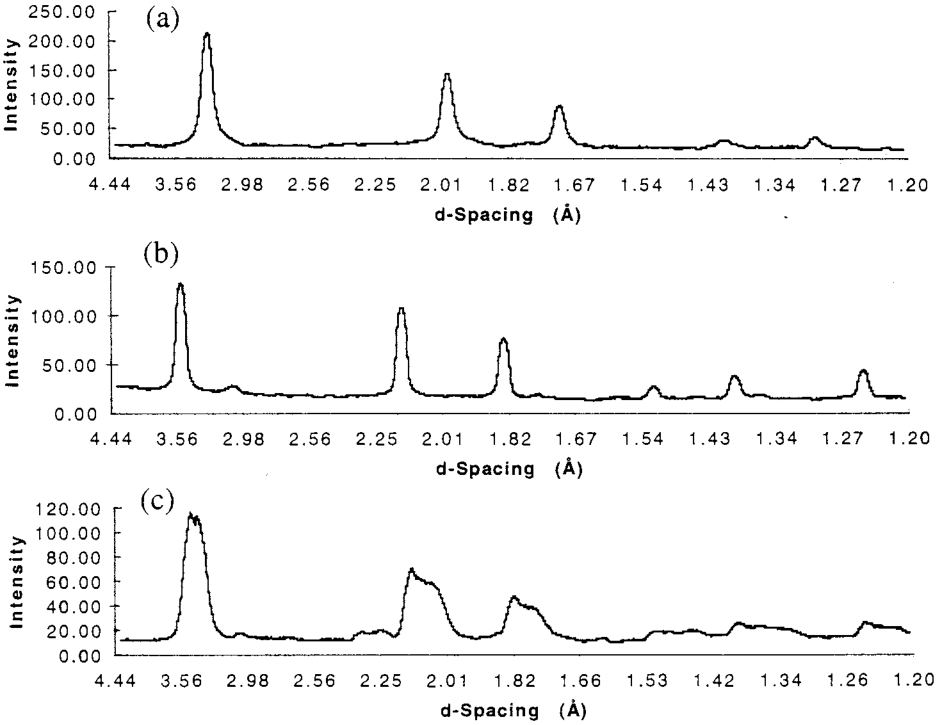

Fig. 4. XRD plots showing: (a) GaAs obtained from the thermolysis of **1** at 400°C; (b) GaSb obtained from the thermolysis of **2** at 400°C; (c) $GaAs_xSb_{(1-x)}$ obtained from the thermolysis of **3** at 400°C.

Examination of the ^{1}H-NMR spectra of **3** also finds it to be more complex than predicted. The $-SiMe_3$ region contains peaks that can be assigned to **1** and **2**, as well as a unique set of peaks that were attributed to **3**. The observed dimer/trimer equilibrium of **2** further complicates the spectra. As the temperature was increased, the peak at δ 0.57 began to lose intensity relative to the peak at δ 0.50. Both of these peaks are assigned to **2** and this behavior is consistent with the observations made during the variable temperature study of **2** (vide supra). In addition, this singlet at δ 0.50 began to coalesce with the singlet at δ 0.51 (assigned to the antimony bound $-SiMe_3$ groups of **3**), with the coalescence occurring at ca. 75°C. Similar behavior was observed with the singlets at δ 0.42 (assigned to the $-SiMe_3$ groups of **1**) and δ 0.41 (assigned to the arsenic bound $-SiMe_3$ groups of **3**), with a coalescence temperature of ca. 95°C. When the sample was cooled to 25°C, all peaks returned to their initial positions and intensities. Based on these spectroscopic observations, it appears that the mixed-pnicogen **3** is in equilibrium with the dimeric **1** and **2**. The temperature of the sample was lowered to 0°C as well, however, no noticeable changes were observed in the spectra.

In order to determine the suitability of **1**, **2** and **3** as precursors to GaAs, GaSb and $GaAs_xSb_{(1-x)}$, respectively, the thermolysis behavior of all three compounds was examined. The temperature used for the pyrolysis was 400°C in all cases. In the case of **1**, the bulk powder produced from the pyrolysis was identified as GaAs by XRD, produced in a 17.5% yield. The approximate average particle size of 9 nm was calculated using the Scherrer equation. The volatiles produced during the thermolysis were trapped and analyzed by IR spectroscopy, and found to be CH_4, ethylene and $HSiMe_3$. The CH_4 produced was too small to measure, and presumably results from secondary decomposition of the condensed gases. The ethylene and $HSiMe_3$ obtained were 20% of the amount expected for complete elimination. These condensed gases are indicative of a β-hydride elimination pathway, where ethylene is eliminated initially, leaving behind a metal–hydride species. This intermediate then eliminates $HSiMe_3$, resulting in formation of the desired material. Elemental analysis of this sample indicates that it is 98.78% GaAs, with a small amount (1.21% total) of residual carbon and hydrogen present, and a Ga:As ratio of 1.00:1.00. For **2**, the GaSb that was obtained amounted to a 20% yield, and the trapped gases (ethylene and trimethylsilane, by IR) accounted for 29% of the total expected for complete elimination. An approximate average particle size of 10 nm was calculated using the Scherrer equation. Full elemental analysis could not be obtained for this material, however the carbon and hydrogen contamination is low (2.03% total), and the gallium analysis is satisfactory. The mixed-pnicogen **3** produces bulk material in an 18% yield, and the XRD plot for the powder indicates that it may contain $GaAs_xSb_{(1-x)}$. This observation is based on the fact that the XRD spectra contains three peaks, each of which lies between values associated with GaAs and GaSb. Such average values are also associated with other compounds believed to be ternary materials [8,9]. The condensed gases given off during the thermolysis of **3** were again identified as ethylene and $HSiMe_3$ by IR, and amounted to 22% of the total expected for complete elimination. Once again, full elemental analysis could not be obtained, but the material exhibits low carbon and hydrogen contamination (1.44% total) and the gallium and arsenic analyses lead to a formula of $GaAs_{0.5}Sb_{0.5}$ by difference. XRD plots for the materials obtained from **1**, **2** and **3** can be found in Fig. 4.

In the thermolysis of these three compounds, it is clear that while relatively clean nanocrystalline material is produced, the overall yields are low, ca. 20% in all cases. One contributing factor to these low yields is the high volatility of compounds **1**, **2** and **3**, all of which sublimed readily under the conditions of the experiment. This volatility, although detrimental to the described studies, suggests that these compounds may be excellent candidates for CVD experiments, and this behavior can be attributed in part to the incorporation of the smaller alkyl group on the gallium. In preliminary studies, we have utilized **2** in the deposition of thin films of GaSb. In addition, the apparent production of $GaAs_xSb_{(1-x)}$ from **3** makes this compound an excellent candidate for such experiments. Further studies on the thermolysis and CVD potential of ethyl containing dimeric and mixed-pnicogen compounds are currently underway.

4. Supplementary Material

Tables of bond distances, bond angles, anisotropic temperature factor parameters, and fractional coordinates for **1**, **2** and **3** have been deposited with the CCDC, CCDC No. 103097 for **1**, CCDC No. 103198 for **2**, CCDC No. 103099 for **3**. Copies of this information may be obtained free of charge from The Director, CCDC, 12 Union Road, Cambridge, CB2 1EZ, UK (Fax: +44-1223-336-033; e-mail: deposit@ccdc.cam.ac.uk or www: http://www.ccdc.cam.ac.uk).

Acknowledgements

The authors wish to thank the Office of Naval Research for their financial support of this work.

References

[1] See the following and the references contained therein: R.L. Wells, W.L. Gladfelter, J. Cluster Sci. 8 (1997) 217.

[2] (a) R.L. Wells, C.G. Pitt, A.T. McPhail, A.P. Purdy, S. Shafieezad, R.B. Hallock, Chem. Mater. 1 (1989) 4. (b) R.L. Wells, M.F. Self, A.T. McPhail, S.R. Aubuchon, R.C. Woudenberg, J.P. Jasinski, Organometallics 12 (1993) 2832. (c) J.F. Janik, R.A. Baldwin, R.L. Wells, W.T. Pennington, G.L. Schimek, A.L. Rheingold, L.M. Liable-Sands, Organometallics 15 (1996) 5385. (d) R.A. Baldwin, E.E. Foos, R.L. Wells, Mat. Res. Bull. 32 (1997) 159.

[3] J.F. Janik, R.L. Wells, Chem. Mater. 8 (1996) 2708.

[4] R.L. Wells, E.E. Foos, P.S. White, A.L. Rheingold, L.M. Liable-Sands, Organometallics 16 (1997) 4771.

[5] A.H. Cowley, R.A. Jones, K.B. Kidd, C.M. Nunn, D.L. Westmoreland, J. Organomet. Chem. 341 (1988) C1.

[6] A.H. Cowley, R.A. Jones, C.M. Nunn, D.L. Westmoreland, Chem. Mater. 2 (1990) 221.

[7] R.A. Baldwin, E.E. Foos, R.L. Wells, P.S. White, A.L. Rheingold, G.P.A. Yap, Organometallics 15 (1996) 5035.

[8] R.L. Wells, S.R. Aubuchon, M.S. Lube, P.S. White, Main Group Chem. 1 (1995) 81.

[9] S.R. Aubuchon, M.S. Lube, R.L. Wells, Chem. Vap. Depos. 1 (1995) 28.

[10] J.A. Laske Cooke, R.L. Wells, P.S. White, Organometallics 14 (1995) 3562.

[11] L.J. Jones, A.T. McPhail, R.L. Wells, Organometallics 13 (1994) 2504.

[12] (a) G. Becker, G. Gutekunst, H.J. Wessely, Z. Anorg. Allg. Chem. 462 (1980) 113. (b) R.L. Wells, M.F. Self, J.D. Johansen, J.A. Laske, S.R. Aubuchan, L.J. Jones, Inorg. Syn. 31 (1997) 150.

[13] E. Amberger, G. Salazar, J. Organomet. Chem. 8 (1967) 111.

[14] H.P. Klug, L.E. Alexander, X-Ray Diffraction Procedures, Wiley, New York, 1962, p. 491.

[15] R.D. Culp, A.H. Cowley, A. Decken, R.A. Jones, M.R. Bond, L.M. Mokry, C.J. Carrano, Inorg. Chem. 36 (1997) 5165.

[16] R.L. Wells, A.T. McPhail, A. Alvanipour, Polyhedron 11 (1992) 839.

[17] R.L. Wells, J.W. Pasterczyk, A.T. McPhail, J.D. Johansen, A. Alvanipour, J. Organomet. Chem. 407 (1991) 17.